



Animal Models of Retinopathy of Prematurity

2

Chi-Hsiu Liu and Jing Chen

Abstract

Retinopathy of prematurity (ROP) is a leading cause of blindness in preterm infants. It is a biphasic disease characterized by an initial phase of arrested vascular growth caused by hyperoxia exposure and loss of maternal–fetal interaction, followed by a second phase of hypoxia-induced neovascularization, which may lead to retinal detachment and vision loss. Animal models of ROP are crucial for studying the cellular and molecular mechanisms underlying ROP pathogenesis and for the development of potential therapeutics. Early animal models of oxygen-induced ROP were developed in the 1950s in multiple species including feline, canine, and murine, after the recognition of supplemental oxygen use as a risk factor. Refined mouse and rat models of oxygen-induced retinopathy were modernized in the 1990s with standardized oxygen protocols and improved methods for assessing retinopathy severity. More recently, murine models of hyperglycemia-associated neonatal retinopathy were developed to mimic neonatal hyperglycemia, a newly identified ROP risk factor. This chapter summarizes the basic concepts, advantages, and limitations of animal models of ROP, with a focus on the most widely used mouse model of oxygen-induced retinopathy.

Keywords

Retinopathy of prematurity · Animal models
Oxygen-induced retinopathy · Vaso-obliteration
Neovascularization

2.1 Introduction

Retinopathy of prematurity (ROP), a potentially blinding disorder caused by abnormal retinal blood vessel growth affecting premature infants, was first reported as “retrolental fibroplasia” by Theodore L. Terry during its epidemic in the 1940s [1]. In the 1930s and 1940s, oxygen administration became a common practice in neonatal care to improve the health of preterm infants with underdeveloped pulmonary function [2, 3]. The epidemic of ROP and ROP-associated blindness soon followed in the 1940s and early 1950s [4], which led to the recognition that unrestricted supplemental oxygen therapy was associated with ROP risk, as initially suggested by Kate Campbell [5] and confirmed by subsequent studies [6, 7]. This discovery of oxygen use as a key risk factor for ROP enabled early development of animal models of ROP in the 1950s. These models recapitulated the detrimental vascular effects of excess oxygen on retinal vascular growth in feline, canine, and murine pups, although inconsistencies remained. Modernization of murine ROP models in the 1990s [8, 9] standardized the protocols of oxygen exposure and methods for evaluation of ROP severity. Combined with the availability of genetically manipulated mice, these newer models greatly advanced research investigating the molecular basis of ROP pathogenesis and the development of potential therapeutics.

Decades of clinical and experimental ROP research have led to the consensus that ROP is a biphasic disease consisting of an initial phase of incomplete retinal vessel growth followed by a second phase of hypoxia-driven pathologic vessel proliferation [10–12]. Unlike full-term infants whose retinal vessels are almost completely developed, infants born prematurely have incompletely developed retinal vasculature with a peripheral avascular zone. After premature birth, the development of retinal vessels is delayed by the relatively hyperoxic postnatal room air environment (compared with in utero) and further worsened by the supplemental oxygen therapy. The first phase of ROP occurs between birth and approximately 30–32 weeks postmenstrual age. As the infant

C.-H. Liu · J. Chen (✉)
Department of Ophthalmology, Boston Children’s Hospital and
Harvard Medical School, Boston, MA, USA
e-mail: Chi-Hsiu.Liu@childrens.harvard.edu; Jing.Chen@childrens.harvard.edu

matures, the peripheral avascular retina becomes increasingly metabolically active, leading to tissue ischemia and hypoxia, which is often exacerbated by the termination of oxygen therapy [13–16]. Hypoxia stimulates upregulation of pro-angiogenic growth factors, such as vascular endothelial growth factor (VEGF) and erythropoietin (EPO), leading to uncontrolled vascular growth into the vitreous, occurring at the junction of avascularized and vascularized retina, and, in severe cases, tractional retinal detachment and blindness [10–12]. The second phase of ROP begins around 32–34 weeks postmenstrual age. Both ROP phases can be closely mimicked in the animal models of oxygen-induced retinopathy (OIR) to allow investigation on the mechanisms of vaso-obliteration, vascular regeneration, and pathological neovascularization processes.

Unlike humans, in whom retinal vessels develop fully before birth, in animal models of feline, canine, and rodent, retinal vessels develop and mature postnatally [16, 17]. Therefore, although these oxygen-induced ROP models reproduce the essential vascular features of ROP, they model only the oxygen influence without taking into account the prematurity itself, which is challenging to model in utero. Factors related to prematurity, such as essential fatty acids and insulin-like growth factors (provided in the third trimester in utero and often decreased or missing after premature birth), are commonly investigated experimentally using supplemental treatments in the OIR model [18, 19]. As additional risk factors (such as neonatal hyperglycemia, a common problem in extremely preterm infants) have been associated with severe ROP [20–23], new murine models of neonatal hyperglycemia-associated retinopathy [24, 25] have also been generated recently. This chapter mainly reviews the historical development of ROP models and focuses primarily on the most commonly used mouse and rat models [8, 9], with a brief discussion of hyperglycemia-associated neonatal retinopathy models [24, 25].

2.2 Experimental Models of ROP

The OIR models have been valuable tools with which to explore the role of oxygen and oxygen-related factors in the pathogenesis of ROP. These models were developed by exposing newborn experimental animals, including feline [26], murine [8, 9], canine [27–29], and piscine (fish) [30], to constantly high or cycling high and low oxygen environments. These animal models of OIR reproduce both the initial vaso-obliteration phase and subsequent ischemia- and hypoxia-induced neovascularization phase, resembling ROP in humans. Due to their simplicity in the induction of pathological neovessels and the ease of monitoring and quantification, the animal models of OIR are widely used for studying the mechanisms and evaluating new therapeutics for treating

the sight-threatening neovascularization in ROP and other ischemic proliferative retinopathies, albeit the consistency and reproducibility of neovascularization vary across different species.

2.2.1 Early Animal Models of OIR: The Feline and Canine Models

In light of the clinical observations linking oxygen with ROP, in the early 1950s Ashton et al. exposed kittens to 70–80% of oxygen for at least 4 days, causing retinal vascular closure and obliteration, then returned them to ambient air (21% oxygen), resulting in hypoxia-induced vaso-proliferation [26, 31]. This feline model of OIR is one of the earliest experimental models establishing the effects of altering oxygen concentration on retinal vascular development [16, 26]. The model successfully mimics the early stages of ROP closely and characterizes both the vaso-obliterative and the vaso-proliferative phases.

Attempts at using the canine OIR model for studying ROP were made at about the same time, in which the first model was developed by Patz's group, to determine the effects of oxygen on the immature retinal vasculature in puppies [29, 32], and modified in subsequent studies [27, 28, 33]. Beagle puppies were exposed to 95–100% of oxygen for 4 days to induce retinopathy. Similar to the kitten model, exposure to hyperoxia arrests the retinal vascular development, causing vaso-obliteration. After moving the puppies from hyperoxia back to room air, the resultant relative hypoxia leads to the vaso-proliferative stage [27, 34]. In addition, retinal detachment, which can be observed in the late, severe stage of human ROP, occurs in the canine but not feline or murine OIR model. Whereas feline and canine models are still occasionally used, achieving a statistically significant number of animals can be challenging. Usage of OIR models in mice and rats has been much more common, largely due to the standardization of the murine models and genetic manipulation in mice since the 1990s.

2.2.2 The Mouse Model of OIR

2.2.2.1 Postnatal Development of Mouse Retinal Vasculature

Mouse retinal vascular development follows similar morphological patterns as in humans [17, 35]. A major difference is the temporally delayed nature of retinal angiogenesis and neuron maturation in mice. In a human fetus, the retinal vasculature develops relatively early during the second trimester, whereas in mice it does not begin to develop until after birth [17, 36, 37]. Therefore, human full-term infants are born with mostly mature retinal vasculature while neona-

tal mice possess underdeveloped vasculature in the eyes in the first few postnatal weeks, allowing studies of physiological and pathological retinal angiogenesis. The development of the mouse retinal vasculature starts with sprouting from the optic nerve head, parallel to the regression of hyaloid vasculature. The hyaloid vasculature is a transient circula-

tory system providing oxygen and nutrient to the developing lens and inner retina as well as the primary vitreous in embryonic eyes [38–40]. During the first postnatal week, the retinal vessels expand radially, forming the superficial vascular plexus; the hyaloid vasculature starts to degenerate at the same time (Fig. 2.1a) [40]. From the second week onward,

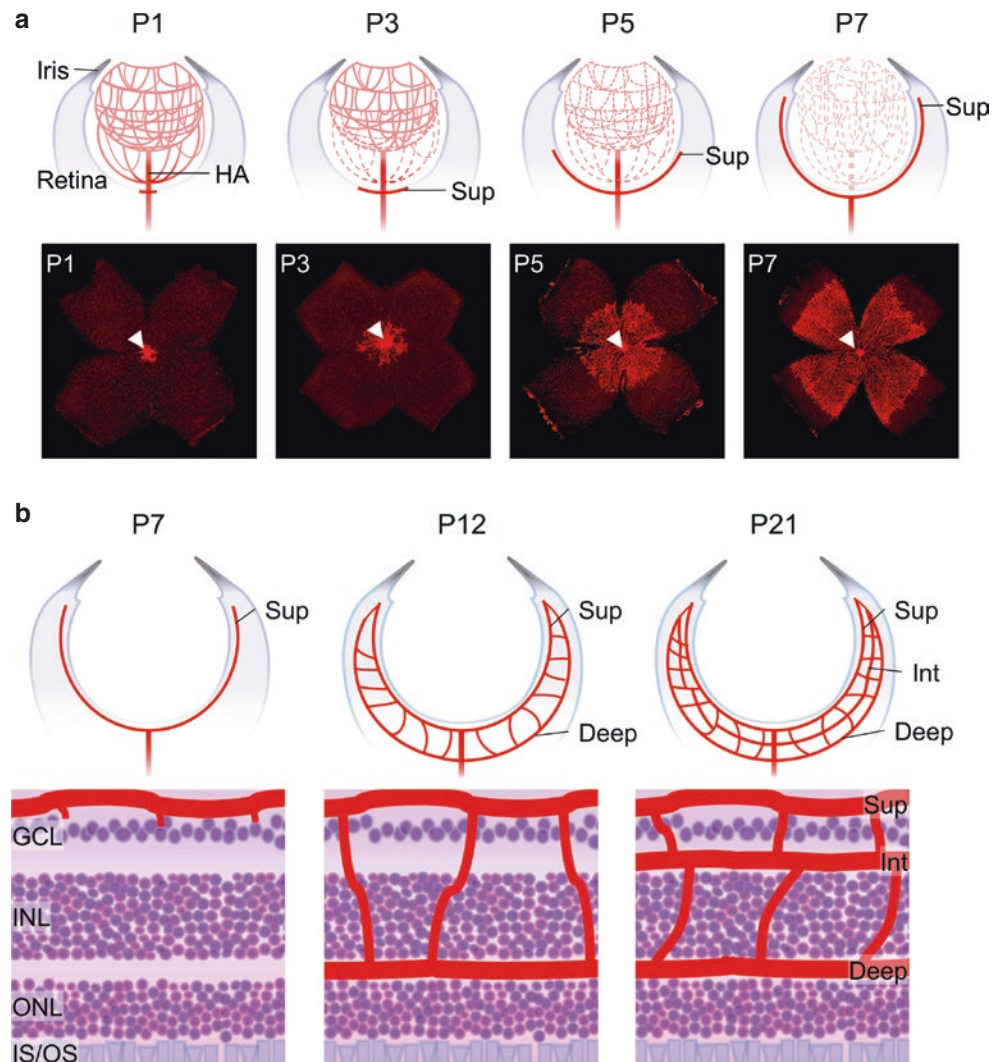


Fig. 2.1 Postnatal development of mouse retina vasculature. (a) Development of mouse retinal vessels occurs postnatally. The upper panels illustrate cross-section diagrams of mouse eyes with developing superficial retinal vascular plexus (Sup; indicated in red) from postnatal day (P) 1 to 7, parallel to regression of hyaloid vasculature (indicated in light red), which is a transient embryonic vascular bed providing blood supply to the developing eye. The lower panels are representative images of the retinal flat mounts from C57BL/6J mice. The vasculature was stained with isolectin (red). At P1, the mouse retina is nearly devoid of blood vessels. Originating from the optic nerve head (white arrowheads), the superficial vascular plexus extends radially from the central retina and reaches the peripheral retina by the end of the first week of postnatal development. (b) Development of the deep and intermediate vascular plexus in mouse retina occurs from the second week postnatally. The upper panels are cartoons of eye cross-sections over-

viewing the organization of three retinal layers (at P7, P12, and P21) during the development of superficial, intermediate, and deep vascular layers. The lower panels are schematic images of retinal cross-sections showing the maturation process of the three retinal vascular plexuses (in red). During the first postnatal week, the superficial plexus reaches out to the edge of the peripheral retina. From the second week onward, the superficial vascular plexus starts to grow perpendicularly into the retina to form the deep vascular plexus between the INL and ONL, which is fully developed at P12. Further growth and maturation of the intermediate plexus continue between the GCL and INL and are mostly complete by P21. Deep, deep retinal vessels; GCL, ganglion cell layer; INL, inner nuclear layer; Int, intermediate retinal vessel; IS/OS, inner segment/outer segment of photoreceptors; ONL, outer nuclear layer; Sup, superficial retinal vessels. The retinal flat mount images in panel a were adapted and reprinted with permission from Stahl et al. [17]

the superficial capillaries grow perpendicularly into the inner retina, forming the deep and then the intermediate vascular plexuses (Fig. 2.1b). By the end of the third postnatal week, a complete retinal vasculature is developed, and hyaloid vessels are mostly regressed [37]. During this period, especially in the first week, the immature retinal vasculature and remnant hyaloid vessels in neonatal mouse pups resemble those of preterm human infants, having a largely avascular retina and highly susceptible to oxygen-induced retinopathy [17].

2.2.2.2 The Mouse OIR Model

In the 1950s, around the same time as the studies in the kitten OIR model, pathologic features resembling ROP were reported in mouse retinas exposed to high oxygen conditions [29, 41]. Subsequent studies in mice further examined the effects of varying oxygen conditions on reproducing ROP-like pathological ocular characteristics [42, 43], providing insights that helped shape the current standardized OIR models.

Coupled with advanced technology in the visualization of retinal vasculature, uniform and thorough assessment of retinopathy severity, as well as the advantage of genetic manipulation in mice, the current mouse model of OIR described by Smith et al. in the 1990s is one of the most commonly used OIR models [9, 44]. In this model, neonatal mice are exposed to $75\% \pm 2\%$ of oxygen for 5 days starting at postnatal day (P) 7, followed by 5 days in room air starting from P12 to P17 (Fig. 2.2a). Hyperoxia conditions from P7 to P12 result in central retinal vessel regression, leading to vaso-obliteration and mimicking the initial stage of ROP. The maximal amount of vessel loss is observed at P9, followed by slow revascularization into the vaso-obliterated areas [45, 46]. After returning to room air at P12, the retinal areas with vaso-obliteration become ischemic and hypoxic, leading to stimulation of hypoxia-induced pro-angiogenic factors, such as VEGF and EPO, resulting in both physiological revascularization of the vaso-obliteration area and also uncontrolled compensatory pathological neovascularization (Fig. 2.2b), resembling the proliferative stage of human ROP [9, 47–50]. These pathological neovessels, also known as preretinal tufts, are disorganized, small-caliber clumps of neovascularization growing at the border between vascular and avascular areas and protruding intravitreally (Fig. 2.2c, d). At P17, the typical endpoint of this mouse model, the extent of pathological neovessels reaches the maximal severity and is also accompanied by increased vascular leakage and breakdown of the blood–retinal barrier. After P17, abnormal preretinal neovascularization starts gradual regression spontaneously and completely disappears by about P25 [44].

The mouse retinal vasculature can be visualized by fluorescent angiography, which highlights the lumen of blood vessels, or (more efficiently) by staining with blood vessel markers such as isolectin in retinal flat mounts. Both meth-

ods allow for easy quantification of pathological vascular features with computer-aided imaging software. Both vaso-obliteration and neovascularization levels can be quantified as a percentage of total retinal areas in flat mounts [44, 51]. Moreover, preretinal neovascular tufts protruding into the vitreous cavity can also be visualized and quantified in cross-sections of eyes [9] (Fig. 2.2d). Vascular permeability can be visualized using fluorescent angiography and quantified by Miles assay [51–55]. Delayed retinal neuronal development or retinal thinning also occurs in OIR, mostly in the inner retina. Overall, the accessibility of genetic manipulation and the consistent and reliable induction of neovascularization make the mouse OIR model a popular one for studying ROP pathogenesis. In addition, OIR is a reliable model for the proliferative aspect of diabetic retinopathy and useful for investigating other diseases related to abnormal neovascularization.

The mouse OIR model reproduces vaso-obliteration and neovascularization consistently, contributing to its broad use in ROP research. Yet one limitation is that the area of vaso-obliteration locates in the central part of the retinas, unlike the peripheral avascular regions in humans. This geographic localization of the peripheral avascular region is recapitulated better in the rat OIR model with cycling oxygen exposure. In addition, there are strain-dependent differences in mouse angiogenic response and hence OIR susceptibility [56, 57]. In general, 129S strains with mixed background are more angiogenic and show higher levels of neovascular response in OIR than inbred C57BL/6 strains do, and the albino BALB/cByJ strain is even less angiogenic than C57BL/6. Moreover, venter-related substrain differences in OIR neovascularization may also exist, even within the same strain [17]. These strain considerations need to be taken into account when choosing appropriate OIR mouse strains.

Another important consideration for interpreting the OIR phenotype is postnatal weight gain of mouse pups during OIR. Postnatal weight gain is a reliable predictor for the severity of clinical ROP in infants [58–60]. Similarly, in the mouse OIR model, pups with poor postnatal weight gain (<5 g at P17) reveal dampened vascular response and prolonged phase of retinopathy compared with medium postnatal weight gain (5 g–7.5 g at P17) and extensive postnatal weight gain (>7.5 g at P17) pups [61]. Monitoring mouse weight gain and keeping them in the normal range is necessary for proper interpretation of OIR data. Runty pups (<5 g) with poor OIR responses should be excluded from data analysis. Other factors, such as the hypoxic effect on lactating mothers [42, 62], may affect maternal care of pups and the susceptibility and severity of the OIR phenotype, hence surrogate mouse mothers may be used when needed.

The mouse OIR model greatly facilitated the investigation of various molecular pathways in developmental and pathological retinal angiogenesis, particularly the discovery of

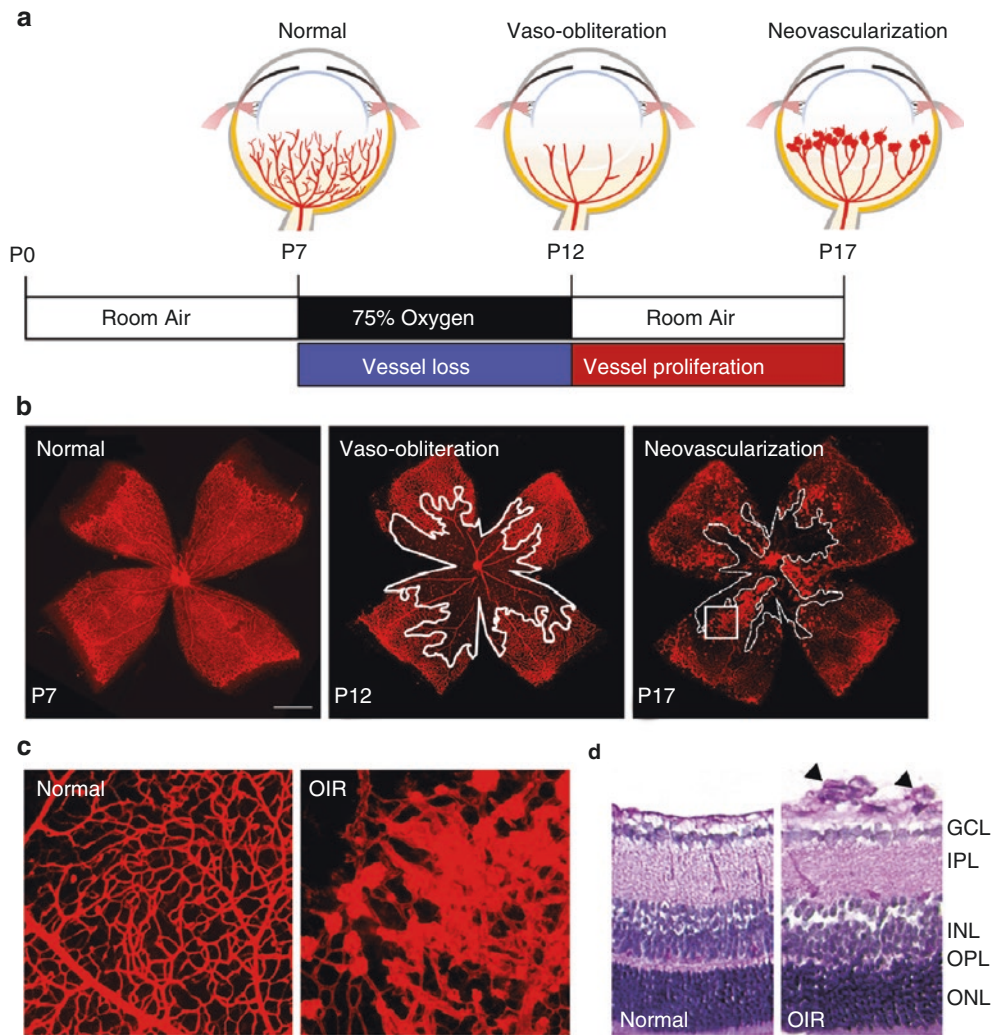


Fig. 2.2 The mouse model of oxygen-induced retinopathy (OIR). (a) A schematic diagram illustrates the procedure of mouse OIR. Neonatal litters are exposed to $75\% \pm 2\%$ oxygen from P7-P12. Hyperoxia suppresses retinal vascular development and leads to the regression of existing immature retinal vessels, resulting in a central zone of vaso-obliteration. At P12, mice are returned to room air, and the relative hypoxia triggers vessel regrowth toward the vaso-obliteration zone as well as pathological neovascularization at the border between the vascular and avascular areas. The levels of neovascularization reach maximum severity at P17. (b) Representative images of retinal flat mounts with isolectin staining (red) in the normoxic and OIR retinas show the normal retinal vasculature at P7 (left panel), vaso-obliteration at P12 (middle panel; the area of vessel loss is outlined in white), and patho-

logic neovascularization at P17 (right panel; the vessel loss area is outlined with a white dashed line). Scale Bar: 1 mm. (c) Magnified images of isolectin-stained retinal flat mounts show the normal vasculature (left panel) from normoxia mice and pathological neovessels in the OIR mouse at P17. Right panel image was enlarged from the rectangular region in (b). (d) Cross-sections of mouse retinas with normoxia (left panel) and OIR (right panel) at P17. The sprouting neovascular tufts (arrows) in the OIR mouse arise from the superficial retinal vascular layer and protrude into the vitreous. GCL, ganglion cell layer; INL, inner nuclear layer; IPL, inner plexiform layer; ONL, outer nuclear layer; OPL, outer plexiform layer. Figure was adapted and reprinted with permission from Liu et al. [36]

VEGF's role in retinopathy. By utilizing the mouse OIR model, previous pioneering studies demonstrated that VEGF induces pathologic retinal neovascularization [49] and that inhibition of VEGF suppresses retinal neovascularization in the OIR mouse eyes [48]. This work, together with studies in other ocular angiogenesis animal models [63–66], laid the experimental foundation for developing current anti-VEGF therapies to treat neovascular age-related macular degenera-

tion and ROP. Besides VEGF, other angiogenic factors, such as EPO [47, 50, 67] and additional signaling pathways, are extensively studied in the OIR model. In addition, factors critical in the third trimester and deficient after preterm birth, such as insulin-like growth factors and omega-3 polyunsaturated fatty acids [18, 19], have also been evaluated utilizing the mouse OIR model (which demonstrated that supplementing these factors is beneficial).

2.2.3 The Rat Model of OIR

The rat model of ROP was first demonstrated by Patz [16] in 1954. In that study, newborn rats were exposed to a constant level of high oxygen concentration (60–80%), resulting in preretinal neovascularization [16]. Subsequent studies using rats exposed to hyperoxia conditions also demonstrated abnormal vaso-proliferation with varying inconsistencies [68, 69]. Over the years, investigators explored and revised protocols for modeling human ROP in more efficient experiment settings [70–72]. Clinical studies revealed that, besides continuous oxygen supplement, oxygen fluctuation also contributes to the incidence of severe ROP [73, 74]. The partial pressure of dissolved arterial oxygen may fluctuate very quickly in premature infants, leading to the alternating occurrence of severe and extended hyperoxemia and hypoxemia [73], which in turn may lead to a higher risk of developing ROP. Based on these observations, Penn and colleagues developed the current rat model, which utilizes alternating hyperoxia–hypoxia cycles, in which the oxygen levels cycle between 50% and 10% every 24 hours for the first 14 days after birth followed by room air exposure through P20 [8, 11, 75] (Fig. 2.3). This rat model recreates oxygen tension fluctuation, which mirrors varying oxygen levels measured in preterm infants developing severe ROP [11], whereas in the mouse model the oxygen level remains constant during continuous oxygen exposure. Exposure to cycling levels of oxygen retards the retinal vascular development, leading to a peripheral avascular zone mimicking human ROP. After returning to room air, neovascular tufts grow at the boundary between vascular and avascular areas in the mid-peripheral retina. One main advantage of the rat OIR model lies in its clinically relevant feature of ROP—delayed development of retinal vasculature followed by pathologic neovascularization. The vaso-obliteration phenotype in the rat OIR model is highly reminiscent of the peripheral avascular zone observed in human ROP, whereas in the mouse model it is the central retinal vessels that are obliterated [76, 77]. Disadvantages of the rat model include lack of genetically modified animals, stain-dependent variation in response, and relatively inconsistent and low levels of neovascularization, which together limit its use in evaluating antiangiogenic therapies.

2.2.4 The Zebrafish Model

The zebrafish, albeit not directly relevant for clinical ROP, is an alternative model for studying angiogenesis-dependent ocular diseases and drug screening [78]. An adult zebrafish model of hypoxia-induced retinopathy was generated [30,

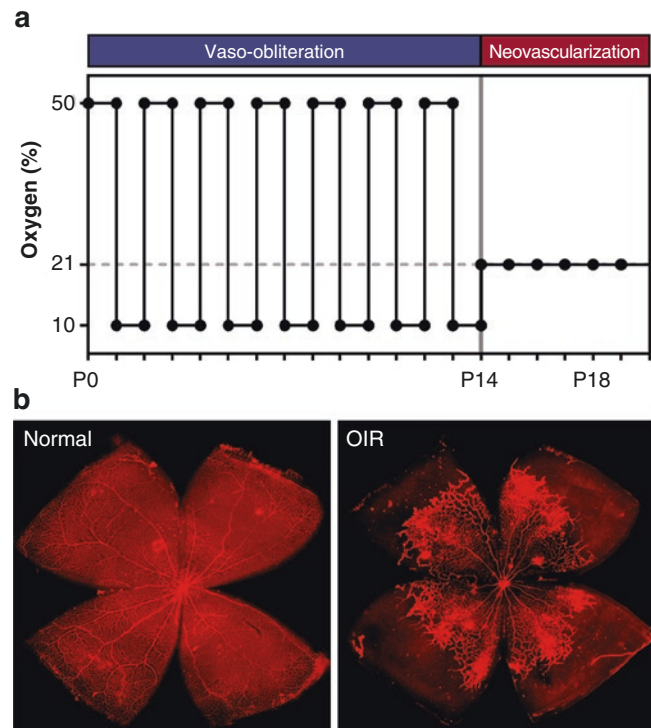


Fig. 2.3 The rat model of oxygen-induced retinopathy (OIR). (a) A schematic illustrates the rat OIR regimen, the 50/10 model. This model exposes neonatal rat litters to alternating 24-hour periods of 50% and 10% oxygen from P0 to P14. After 14 days of variable oxygen, rats are returned to room air (21% oxygen), inducing the development of neovascularization. (b) Representative retinal flat mount images of normoxic and the 50/10 OIR rat retinas. Retinas were collected from P18 normal (left panel) and OIR (right panel) rats followed by isolectin-staining to visualize the vasculature. Rat retinas with OIR show delayed vascular development in the peripheral area with a vaso-obliterated zone and neovascularization at the boundary of vascular and avascular areas. Panel b: Image courtesy of Dr. James D. Akula, Boston Children’s Hospital, Harvard Medical School, Boston, MA, USA

79], utilizing blood vessel-specific stable fluorescent reporter transgenic zebrafish [80, 81]. When placed in a hypoxic aquarium with 10% air saturation (820 parts per billion) for 3–12 days, new retinal vessel sprouts reached a plateau of maximal angiogenic responses at day 12 [30, 79]. Subsequently, an embryonic model of ROP was also developed using hypoxia-inducing chemical agents to stimulate abnormal retinal angiogenesis in zebrafish embryos [82].

2.2.5 Hyperglycemia-Associated ROP Models

Neonatal hyperglycemia, common in extremely preterm infants, has been recognized as an ROP risk factor [20–23]. Neonatal hyperglycemia often occurs in preterm infants receiving glucose infusion and is related to incomplete sup-

pression of hepatic glucose production after infusion, inadequate pancreatic beta-cell response, and insulin insensitivity [83–86]. A hyperglycemia-associated retinopathy model was generated in neonatal rats by using a single injection of streptozotocin (STZ) at P1 [24]. Sustained hyperglycemia was induced rapidly from P2/3 to P6, and retinal angiogenesis is inhibited, with associated inflammatory response and inner retinal neuron degeneration within 2 weeks postnatally [24]. Recently, a similar mouse model of hyperglycemia-associated ROP was developed with daily injections of STZ from P1 to P9. Hyperglycemia was induced at P8, followed by delayed deep layer retinal vessel growth and photoreceptor dysfunction [25]. Together these models recapitulate delayed vascular development of ROP and may help elucidate the mechanisms of hyperglycemia-induced retinal damage in ROP.

2.3 Summary

ROP remains a leading cause of visual impairment and a challenge in neonatology worldwide. Animal models of ROP have evolved over the past several decades with vast amounts of research efforts directed toward better understanding of the pathogenesis of ROP, especially in the mechanisms governing retinal angiogenesis. The establishment of different experimental models allows investigators to explore the roles that many influencing factors (e.g., oxygen, light conditions, and hyperglycemia) play in ROP development. For instance, studies from the early feline, canine, and murine models of ROP provided compelling evidence that high levels of oxygen promoted obliteration of blood vessels in the developing retina [29, 69], suggesting the importance of titrating and close monitoring of exogenous oxygen administration to the preterm infants. Insights on an essential role of VEGF in ROP development were also derived from studies in OIR models, which facilitated the development of current anti-VEGF therapies.

Among several different species, the mouse model of OIR is the most representative model for studying ROP and other ocular diseases involving hypoxia-induced angiogenesis. As of December 2018, there are more than 700 PubMed publications using the mouse OIR model of ROP. These studies reflect the broad value of the mouse OIR model for studying mechanisms underlying pathological angiogenesis in retinal and tissue ischemia, including the roles of growth factors, fatty acids, inflammation, signaling cascades, metabolic and transcriptional regulation, and regulatory non-coding RNAs on ROP. In addition, the mouse OIR model, with its fast induction of consistent neovascularization, is also extensively used in evaluating antiangiogenic drugs, to facilitate the development of new therapies for ROP and other vascular eye disorders.

References

1. Terry TL. Fibroblastic overgrowth of persistent tunica vasculosa lentis in infants born prematurely: II. Report of cases-clinical aspects. *Trans Am Ophthalmol Soc.* 1942;40:262–84.
2. Coats DK. Retinopathy of prematurity: involution, factors predisposing to retinal detachment, and expected utility of preemptive surgical reoperation. *Trans Am Ophthalmol Soc.* 2005;103:281–312.
3. Hess JH. Oxygen unit for premature and very young infants. *Am J Dis Chil.* 1934;47:916–7.
4. Silverman WA. *Retrolental fibroplasia: a modern parable.* New York: Grune & Stratton; 1980.
5. Campbell K. Intensive oxygen therapy as a possible cause of retrolental fibroplasia; a clinical approach. *Med J Aust.* 1951;2:48–50.
6. Patz A, Hoeck LE, De La Cruz E. Studies on the effect of high oxygen administration in retrolental fibroplasia I. Nursery observations. *Am J Ophthalmol.* 1952;35:1248–53.
7. Kinsey VE. Retrolental fibroplasia; cooperative study of retrolental fibroplasia and the use of oxygen. *AMA Arch Ophthalmol.* 1956;56:481–543.
8. Penn JS, Tolman BL, Lowery LA. Variable oxygen exposure causes preretinal neovascularization in the newborn rat. *Invest Ophthalmol Vis Sci.* 1993;34:576–85.
9. Smith LE, et al. Oxygen-induced retinopathy in the mouse. *Invest Ophthalmol Vis Sci.* 1994;35:101–11.
10. Chen J, Smith LE. Retinopathy of prematurity. *Angiogenesis.* 2007;10:133–40.
11. Hartnett ME, Penn JS. Mechanisms and management of retinopathy of prematurity. *N Engl J Med.* 2012;367:2515–26.
12. Hellstrom A, Smith LE, Dammann O. Retinopathy of prematurity. *Lancet.* 2013;382:1445–57.
13. Hardy P, et al. Oxidants, nitric oxide and prostanoids in the developing ocular vasculature: a basis for ischemic retinopathy. *Cardiovasc Res.* 2000;47:489–509.
14. Schaffer DB, The Cryotherapy for Retinopathy of Prematurity Cooperative Group, et al. Prognostic factors in the natural course of retinopathy of prematurity. *Ophthalmology.* 1993;100:230–7.
15. Foos RY. Chronic retinopathy of prematurity. *Ophthalmology.* 1985;92:563–74.
16. Patz A. Oxygen studies in retrolental fibroplasia. IV. Clinical and experimental observations. *Am J Ophthalmol.* 1954;38:291–308.
17. Stahl A, et al. The mouse retina as an angiogenesis model. *Invest Ophthalmol Vis Sci.* 2010;51:2813–26.
18. Connor KM, et al. Increased dietary intake of omega-3 polyunsaturated fatty acids reduces pathological retinal angiogenesis. *Nat Med.* 2007;13:868–73.
19. Smith LE, et al. Regulation of vascular endothelial growth factor-dependent retinal neovascularization by insulin-like growth factor-1 receptor. *Nat Med.* 1999;5:1390–5.
20. Garg R, Agthe AG, Donohue PK, Lehmann CU. Hyperglycemia and retinopathy of prematurity in very low birth weight infants. *J Perinatol.* 2003;23:186–94.
21. Blanco CL, Baillargeon JG, Morrison RL, Gong AK. Hyperglycemia in extremely low birth weight infants in a predominantly Hispanic population and related morbidities. *J Perinatol.* 2006;26:737–41.
22. Kaempf JW, et al. Hyperglycemia, insulin and slower growth velocity may increase the risk of retinopathy of prematurity. *J Perinatol.* 2011;31:251–7.
23. Mohamed S, Murray JC, Dagle JM, Colaizy T. Hyperglycemia as a risk factor for the development of retinopathy of prematurity. *BMC Pediatr.* 2013;13:78.
24. Kermorvant-Duchemin E, et al. Neonatal hyperglycemia inhibits angiogenesis and induces inflammation and neuronal degeneration in the retina. *PLoS One.* 2013;8:e79545.

25. Fu Z, et al. Photoreceptor glucose metabolism determines normal retinal vascular growth. *EMBO Mol Med.* 2018;10:76–90.
26. Ashton N, Ward B, Serpell G. Effect of oxygen on developing retinal vessels with particular reference to the problem of retrolental fibroplasia. *Br J Ophthalmol.* 1954;38:397–432.
27. McLeod DS, Brownstein R, Luty GA. Vaso-obliteration in the canine model of oxygen-induced retinopathy. *Invest Ophthalmol Vis Sci.* 1996;37:300–11.
28. Flower RW, Blake DA. Retrolental fibroplasia: evidence for a role of the prostaglandin cascade in the pathogenesis of oxygen-induced retinopathy in the newborn beagle. *Pediatr Res.* 1981;15:1293–302.
29. Patz A, Eastham A, Higginbotham DH, Kleh T. Oxygen studies in retrolental fibroplasia. II. The production of the microscopic changes of retrolental fibroplasia in experimental animals. *Am J Ophthalmol.* 1953;36:1511–22.
30. Cao R, Jensen LD, Soll I, Hauptmann G, Cao Y. Hypoxia-induced retinal angiogenesis in zebrafish as a model to study retinopathy. *PLoS One.* 2008;3:e2748.
31. Phelps DL, Rosenbaum AL. Effects of marginal hypoxemia on recovery from oxygen-induced retinopathy in the kitten model. *Pediatrics.* 1984;73:1–6.
32. Kimura T, Chen CH, Patz A. Light and electron microscopic studies of intravitreal proliferative tissues in human and puppy eyes (author's transl). *Nippon Ganka Gakkai Zasshi.* 1979;83:255–65.
33. McLeod DS, Crone SN, Luty GA. Vasoproliferation in the neonatal dog model of oxygen-induced retinopathy. *Invest Ophthalmol Vis Sci.* 1996;37:1322–33.
34. McLeod DS, Luty GA. Targeting VEGF in canine oxygen-induced retinopathy – a model for human retinopathy of prematurity. *Eye Brain.* 2016;8:55–65.
35. Young RW. Cell differentiation in the retina of the mouse. *Anat Rec.* 1985;212:199–205.
36. Liu CH, Wang Z, Sun Y, Chen J. Animal models of ocular angiogenesis: from development to pathologies. *FASEB J.* 2017;31:4665–81.
37. Chen J, Liu CH, Sapieha P. Anti-angiogenic therapy. In: Stahl A, editor. *Ophthalmology.* Cham: Springer; 2016. p. 1–19.
38. Fruttiger M. Development of the retinal vasculature. *Angiogenesis.* 2007;10:77–88.
39. Hartnett ME. *Pediatric retina.* London: Lippincott Williams & Wilkins; 2013.
40. Ito M, Yoshioka M. Regression of the hyaloid vessels and pupillary membrane of the mouse. *Anat Embryol (Berl).* 1999;200:403–11.
41. Gyllenstein LJ, Hellstrom BE. Retrolental fibroplasia; animal experiments: the effect of intermittently administered oxygen on the postnatal development of the eyes of fullterm mice. *Acta Paediatr.* 1952;41:577–82.
42. Gerschman R, Nadig PW, Snell AC Jr, Nye SW. Effect of high oxygen concentrations on eyes of newborn mice. *Am J Phys.* 1954;179:115–8.
43. Curley FJ, Habegger H, Ingalls TH, Philbrook FR. Retinopathy of immaturity in the newborn mouse after exposure to oxygen imbalances. *Am J Ophthalmol.* 1956;42:377–92.
44. Connor KM, et al. Quantification of oxygen-induced retinopathy in the mouse: a model of vessel loss, vessel regrowth and pathological angiogenesis. *Nat Protoc.* 2009;4:1565–73.
45. Lange C, et al. Kinetics of retinal vaso-obliteration and neovascularisation in the oxygen-induced retinopathy (OIR) mouse model. *Graefes Arch Clin Exp Ophthalmol.* 2009;247:1205–11.
46. Gu X, et al. Effects of sustained hyperoxia on revascularization in experimental retinopathy of prematurity. *Invest Ophthalmol Vis Sci.* 2002;43:496–502.
47. Chen J, Connor KM, Aderman CM, Smith LE. Erythropoietin deficiency decreases vascular stability in mice. *J Clin Invest.* 2008;118:526–33.
48. Aiello LP, et al. Suppression of retinal neovascularization in vivo by inhibition of vascular endothelial growth factor (VEGF) using soluble VEGF-receptor chimeric proteins. *Proc Natl Acad Sci U S A.* 1995;92:10457–61.
49. Pierce EA, Avery RL, Foley ED, Aiello LP, Smith LE. Vascular endothelial growth factor/vascular permeability factor expression in a mouse model of retinal neovascularization. *Proc Natl Acad Sci U S A.* 1995;92:905–9.
50. Chen J, et al. Suppression of retinal neovascularization by erythropoietin siRNA in a mouse model of proliferative retinopathy. *Invest Ophthalmol Vis Sci.* 2009;50:1329–35.
51. Stahl A, et al. Computer-aided quantification of retinal neovascularization. *Angiogenesis.* 2009;12:297–301.
52. Vahatupa M, et al. Lack of R-Ras Leads to Increased Vascular Permeability in Ischemic Retinopathy. *Invest Ophthalmol Vis Sci.* 2016;57:4898–909.
53. Chen J, Stahl A, Hellstrom A, Smith LE. Current update on retinopathy of prematurity: screening and treatment. *Curr Opin Pediatr.* 2011;23:173–8.
54. Fulton AB, et al. Retinal degenerative and hypoxic ischemic disease. *Doc Ophthalmol.* 2009;118:55–61.
55. Xu Q, Qaum T, Adamis AP. Sensitive blood-retinal barrier breakdown quantitation using Evans blue. *Invest Ophthalmol Vis Sci.* 2001;42:789–94.
56. Chan CK, et al. Differential expression of pro- and antiangiogenic factors in mouse strain-dependent hypoxia-induced retinal neovascularization. *Lab Invest.* 2005;85:721–33.
57. Ritter MR, et al. Myeloid progenitors differentiate into microglia and promote vascular repair in a model of ischemic retinopathy. *J Clin Invest.* 2006;116:3266–76.
58. Wallace DK, Kylstra JA, Phillips SJ, Hall JG. Poor postnatal weight gain: a risk factor for severe retinopathy of prematurity. *J AAPOS.* 2000;4:343–7.
59. Allegaert K, et al. Perinatal growth characteristics and associated risk of developing threshold retinopathy of prematurity. *J AAPOS.* 2003;7:34–7.
60. Lofqvist C, et al. Longitudinal postnatal weight and insulin-like growth factor I measurements in the prediction of retinopathy of prematurity. *Arch Ophthalmol.* 2006;124:1711–8.
61. Stahl A, et al. Postnatal weight gain modifies severity and functional outcome of oxygen-induced proliferative retinopathy. *Am J Pathol.* 2010;177:2715–23.
62. Gole GA, Browning J, Elts SM. The mouse model of oxygen-induced retinopathy: a suitable animal model for angiogenesis research. *Doc Ophthalmol.* 1990;74:163–9.
63. Miller JW, et al. Vascular endothelial growth factor/vascular permeability factor is temporally and spatially correlated with ocular angiogenesis in a primate model. *Am J Pathol.* 1994;145:574–84.
64. Shima DT, et al. Cloning and mRNA expression of vascular endothelial growth factor in ischemic retinas of *Macaca fascicularis*. *Invest Ophthalmol Vis Sci.* 1996;37:1334–40.
65. Adamis AP, et al. Inhibition of vascular endothelial growth factor prevents retinal ischemia-associated iris neovascularization in a nonhuman primate. *Arch Ophthalmol.* 1996;114:66–71.
66. Krzystolik MG, et al. Prevention of experimental choroidal neovascularization with intravitreal anti-vascular endothelial growth factor antibody fragment. *Arch Ophthalmol.* 2002;120:338–46.
67. Watanabe D, et al. Erythropoietin as a retinal angiogenic factor in proliferative diabetic retinopathy. *N Engl J Med.* 2005;353:782–92.
68. Brands KH, Hofmann H, Klees E. Not Available. *Geburtshilfe Frauenheilkd.* 1958;18:805–14.
69. Ashton N, Blach R. Studies on Developing Retinal Vessels Viii. Effect of Oxygen on the Retinal Vessels of the Ratling. *Br J Ophthalmol.* 1961;45:321–40.
70. Ricci B, Calogero G. Oxygen-induced retinopathy in newborn rats: effects of prolonged normobaric and hyperbaric oxygen supplementation. *Pediatrics.* 1988;82:193–8.

71. Penn JS, Tolman BL, Lowery LA, Koutz CA. Oxygen-induced retinopathy in the rat: hemorrhages and dysplasias may lead to retinal detachment. *Curr Eye Res.* 1992;11:939–53.
72. Ventresca MR, Gonder JR, Tanswell AK. Oxygen-induced proliferative retinopathy in the newborn rat. *Can J Ophthalmol.* 1990;25:186–9.
73. York JR, Landers S, Kirby RS, Arbogast PG, Penn JS. Arterial oxygen fluctuation and retinopathy of prematurity in very-low-birth-weight infants. *J Perinatol.* 2004;24:82–7.
74. Cunningham S, Fleck BW, Elton RA, McIntosh N. Transcutaneous oxygen levels in retinopathy of prematurity. *Lancet.* 1995;346:1464–5.
75. Penn JS, Rajaratnam VS, Collier RJ, Clark AF. The effect of an angiostatic steroid on neovascularization in a rat model of retinopathy of prematurity. *Invest Ophthalmol Vis Sci.* 2001;42:283–90.
76. Madan A, Penn JS. Animal models of oxygen-induced retinopathy. *Front Biosci.* 2003;8:d1030–43.
77. Grossniklaus HE, Kang SJ, Berglin L. Animal models of choroidal and retinal neovascularization. *Prog Retin Eye Res.* 2010;29:500–19.
78. Rezzola S, Paganini G, Semeraro F, Presta M, Tobia C. Zebrafish (*Danio rerio*) embryo as a platform for the identification of novel angiogenesis inhibitors of retinal vascular diseases. *Biochim Biophys Acta.* 2016;1862:1291–6.
79. Cao Z, et al. Hypoxia-induced retinopathy model in adult zebrafish. *Nat Protoc.* 2010;5:1903–10.
80. Alvarez Y, et al. Genetic determinants of hyaloid and retinal vasculature in zebrafish. *BMC Dev Biol.* 2007;7:114.
81. Weinstein BM, Stemple DL, Driever W, Fishman MC. Gridlock, a localized heritable vascular patterning defect in the zebrafish. *Nat Med.* 1995;1:1143–7.
82. Wu YC, et al. Hypoxia-induced retinal neovascularization in zebrafish embryos: a potential model of retinopathy of prematurity. *PLoS One.* 2015;10:e0126750.
83. Cowett RM, Rapoza RE, Gelardi NL. The contribution of glucose to neonatal glucose homeostasis in the lamb. *Metabolism.* 1998;47:1239–44.
84. Mitanchez-Mokhtari D, et al. Both relative insulin resistance and defective islet beta-cell processing of proinsulin are responsible for transient hyperglycemia in extremely preterm infants. *Pediatrics.* 2004;113:537–41.
85. Cowett RM, Oh W, Schwartz R. Persistent glucose production during glucose infusion in the neonate. *J Clin Invest.* 1983;71:467–75.
86. Sunehag A, Gustafsson J, Ewald U. Very immature infants (< or = 30 Wk) respond to glucose infusion with incomplete suppression of glucose production. *Pediatr Res.* 1994;36:550–5.